The 2010 IEEE/RSJ International Conference on
Intelligent Robots and Systems
October 18-22, 2010, Taipei, Taiwan

Ground reaction force control at each foot: A momentum-based humanoid balance controller for non-level and non-stationary ground

Sung-Hee Lee and Ambarish Goswami

***Abstract*— We present a novel momentum-based method for maintaining balance of humanoid robots. By controlling the desired ground reaction force (GRF) and center of pressure (CoP) at each support foot, our method can naturally deal with non-level and non-stationary ground at each foot-ground contact, as well as different frictional properties. We do not make use of the net GRF and CoP which may be difficult or impossible to compute for non-level grounds. Our method minimizes the ankle torques during double support. We show the effectiveness of this new balance control method by simulating various experiments with a humanoid robot including maintaining balance when two feet are on separate moving supports with different inclinations and velocities.**

***Index Terms*— Humanoid robot balance, linear and angular momentum, non-level ground, centroidal momentum matrix.**

I. Introduction

Even after several decades of intense activity, balance maintenance remains as one of the most fundamental issues of humanoid robot research. Starting from the early work of [1], researchers have developed various approaches, such as joint (e.g., ankle or hip) control strategies [2], [3], whole body control strategies [4], [5], [6], [7], [8], and the methods that find optimal control policies [9].

Except for a few notable exceptions [2], [6] most techniques for humanoid balance and motion have focused on controlling only the linear motion of the robot while ignoring its rotational motion. In these methods a robot is controlled to maintain its center of mass (CoM) along a desired trajectory while restricting its center of pressure (CoP) to remain inside the support base.

However, rotational dynamics of a robot also plays a significant role in balance [10]. In fact, complete control of CoP, which is one of the most important indicators for balance, is impossible without also controlling the angular momentum. This will be evident from the following discussion. The rate of change of linear momentum $\dot{\boldsymbol{l}}$ and the angular momentum $\dot{\boldsymbol{k}}$ about the robot CoM (hence dubbed *centroidal* angular momentum in this paper) of a humanoid robot are related to the GRF $\boldsymbol{f}$ and CoP location $\boldsymbol{p}$ as follows (Fig. 1):

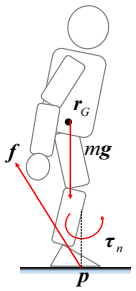

Fig. 1: External Forces

$$\dot{\boldsymbol{l}} = m\boldsymbol{g} + \boldsymbol{f} \quad (1)$$

$$\dot{\boldsymbol{k}} = (\boldsymbol{p} - \boldsymbol{r}_G) \times \boldsymbol{f} + \boldsymbol{\tau}_n \quad (2)$$

S.-H. Lee is with the School of Information and Communications, Gwangju Institute of Science and Technology, South Korea shl@gist.ac.kr. This work was done while SHL was at Honda Research Institute.

A. Goswami is with Honda Research Institute, Mountain View, CA, USA agoswami@honda-ri.com

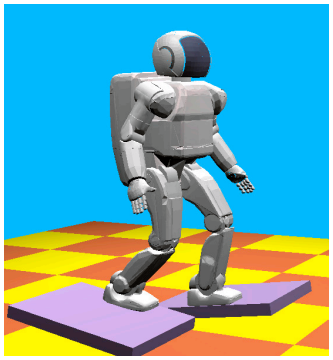
Fig. 2: Our momentum-based controller can maintain balance of humanoid robot on non-level (but locally flat) and non-stationary ground, under various disturbance forces.

where m is the total mass, $\boldsymbol{r}_G$ is CoM location, and $\boldsymbol{\tau}_n$ is the normal ground reaction torque at the CoP. Together $\boldsymbol{l}$ and $\boldsymbol{k}$ is called the spatial centroidal momentum, or in this paper, simply spatial momentum $\boldsymbol{h} = (\boldsymbol{k}, \boldsymbol{l})$ of the robot.

Obviously, as noted by [11], the rate of change of spatial momentum has a one-to-one relationship with the GRF and CoP. Whereas $\dot{\boldsymbol{l}}$ is completely determined by $\boldsymbol{f}$ and vice versa, CoP location $\boldsymbol{p}$, depends on both $\dot{\boldsymbol{l}}$ and $\dot{\boldsymbol{k}}$. Equivalently, $\dot{\boldsymbol{k}}$ depends on both $\boldsymbol{f}$ and $\boldsymbol{p}$. Due to this fact, attempts to control CoP by controlling only CoM trajectory [5], i.e., only linear momentum while ignoring the angular momentum, are fundamentally incomplete. Indeed, experiments on human balance control also show that humans tightly regulate angular momentum during gait [12], which suggests the importance of controlling angular momentum.

In this paper, we present a new method for humanoid balance maintenance that controls both the linear and angular components of the spatial momentum. We first define the *desired* rates of changes of linear and angular momenta that are necessary to maintain balance, and subsequently compute their *admissible* values under the constraints of ground friction and foot contact maintenance. Finally, joint torques are computed using inverse dynamics to generate the admissible momenta rate changes.

Desired momenta are realized by controlling the ground reaction forces. When only one foot is in contact with the ground, the desired support foot GRF is uniquely determined from the desired linear and angular momenta rate changes. However, for double support, there can be infinitely many combinations of individual "foot" GRFs that can create the desired momenta rate changes.

One seemingly straightforward way to deal with this redundancy is by extending the method used for the single support case: first determine the net GRF and CoP, and

then *somehow* resolve them for each foot. This approach, however, has a few drawbacks. Computing a net CoP when each foot rests on different non-level surfaces may or may not be possible. Furthermore, it is difficult to handle the case where each foot is contacting grounds with different velocities and friction properties.

Therefore, in this paper, we present a novel method to compute the individual *foot* GRF and *foot* CoP such that they create the admissible spatial momentum rate change which is the closest possible to the desired value. By directly dealing with each foot separately, we do not need to compute the 3D convex hull of the contact points and can deal with different ground friction at each foot.

The proposed method computes the foot GRFs and CoPs such that they minimize ankle torques while generating desired rates of changes of momenta. This is achieved by solving two constrained linear least-squares problems. Minimizing ankle torque is important because typically the ankle torque is more constrained than others in that it should not cause foot tipping.

We perform various simulation experiments on our balance controller with a humanoid robot model including pushing the single or double-supported robot in various directions and maintaining balance when two feet are on separate moving supports with different inclinations and velocities.

II. Related Work

Although valuable research by Sano and Furusho [2] was performed as early as 1990, the importance of angular momentum for balance maintenance started to be seriously explored much later [6], [13], [12]. Kajita et al. [6] included angular momentum criteria into the whole body balance control framework. Komura et al. [10] presented a balance controller that can counteract rotational perturbations using angular momentum inducing inverted pendulum model (AMPM) which augments the 3D Linear Inverted Pendulum Model (LIPM) [14] with the additional capability of possessing centroidal angular momentum. Naksuk et al. [15] considered angular momentum criteria for trajectory generation of humanoid robots. Abdallah and Goswami [16], and Macchietto et al. [11] defined balance control objectives in terms of CoM and CoP, and achieved this goal by controlling the rates of change of linear and angular momenta of the robot. Hofmann et al. [17] presented a momentum-balance controller that gives higher priority to linear momentum over angular momentum.

Like [6], [16], [11], [17], we also control both the linear and angular components of the spatial momentum of the robot for balance maintenance. However, our method differs from that of [6], which does not check for the admissibility of the desired values of linear and angular momenta, and from [16], [11] which define the balance control objectives in terms of CoM and CoP and not directly in terms of linear and angular momenta. Additionally, our method computes contact forces at each support foot, and therefore can be used both during double-support and single-support and also on non-level ground and non-stationary grounds, whereas [16], [11], [17] consider only single-support.

Regarding the computation of individual foot GRFs and CoPs, Hyon et al. [18] presented a method to minimize the sum of the squared norm of forces at sample contact points while satisfying the desired net GRF and CoP. This method can minimize each foot GRF if the sample contact points are well distributed. Our method also minimizes foot GRFs but puts higher priority to minimizing ankle torques, i.e., keeping foot CoPs below ankles.

III. Momentum-based Balance Control

We describe our momentum-based balance controller in this section. Fig. 3 shows the block diagram of our balance controller. The joint torques are determined through the following steps. We first specify the desired rates of changes of linear and angular momenta for balance (Sec. III-A), and then determine the corresponding foot GRF and foot CoP (Sec. III-B). The admissible momenta rate changes corresponding to physically realizable foot GRF and CoP are computed as well. Next, we resolve the joint accelerations that will satisfy the admissible momenta rate changes as well as the foot contact constraint. Finally we compute necessary joint torques to create the joint accelerations and the external forces using inverse dynamics (Sec. III-C). Each step will be detailed now.

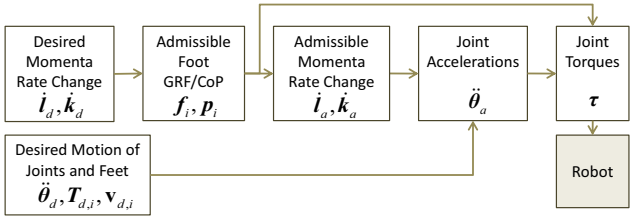

Fig. 3: Controller Block Diagram

A. Desired Momenta for Balance Maintenance

Some balance controllers define the balance control objectives in terms of CoP [16], [11] while others use momenta [6]. Although the rate of change of spatial momentum has a one-to-one relationship with GRF and CoP, their significance regarding balance are different. Whereas the former relates to robot motion, the latter characterizes the nature and constraints of the ground contact. Since the friction values and the unilateral nature of the robot-ground contact limit the allowable range of external forces, the GRF and CoP impose important constraints on achievable range of momenta rate change. Therefore, we use the momenta as control objectives whereas GRF and CoP are used as constraints for verifying the physical realizability of the forces.

The overall behavior of the balance controller against external perturbations is determined by the desired spatial momentum rate change. We employ the following control policy:

$$\dot{\boldsymbol{l}}_d/m = \boldsymbol{\Gamma}_{11}(\dot{\boldsymbol{r}}_{G,d} - \dot{\boldsymbol{r}}_G) + \boldsymbol{\Gamma}_{12}(\boldsymbol{r}_{G,d} - \boldsymbol{r}_G) \quad (3)$$

$$\dot{\boldsymbol{k}}_d = \boldsymbol{\Gamma}_{21}(\boldsymbol{k}_d - \boldsymbol{k}) \quad (4)$$

where $\dot{\boldsymbol{l}}_d$ and $\dot{\boldsymbol{k}}_d$ are desired rate of change of linear and centroidal angular momentum, respectively, $\boldsymbol{r}_{G,d}$ is the desired CoM. $\boldsymbol{\Gamma}_{ij} = \mathrm{diag}(\gamma_{ij})$ is the 3×3 feedback gain parameter matrix. Equations (3) and (4) try to achieve desired CoM trajectory, linear momentum, and angular momentum. For postural balance experiments we set $\boldsymbol{k}_d$ to zero and set the horizontal components of $\boldsymbol{r}_{G,d}$ to the mid-point of the geometric centers of the two feet. For other cases, these values may be determined from the desired motion. Note that we do not have angular position feedback in (4) because there is no "position" corresponding to angular momentum. $\dot{\boldsymbol{l}}_d$ and $\dot{\boldsymbol{k}}_d$ will be used to determine admissible foot GRF and CoP in the next step.

B. Foot GRF and CoP of Each Support Foot

The desired momentum rate changes in (3) and (4) may not necessarily be admissible. Generating them might require the GRF to be outside the friction cone or the CoP to exit the foot support area. Therefore, in the next step, we determine admissible external forces such that the resulting momentum rate changes are as close as possible to the desired values.

While GRF and CoP are uniquely determined from the desired rates of changes of linear and angular momenta during single support, there can be infinitely many solutions for double support. Hence we consider each case separately.

1) Single Support Case: When GRF and CoP computed from the desired momentum rate change (eqs. (1) and (2)) are admissible, we can directly use them. If not, it means that we cannot simultaneously satisfy both $\dot{\boldsymbol{l}}_d$ and $\dot{\boldsymbol{k}}_d$, and hence we need to find an optimal GRF and CoP that will create admissible momentum rate change as close as possible to the desired values.

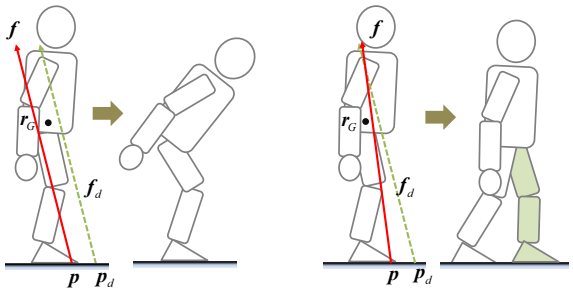

Fig. 4: When $\boldsymbol{p}_d$, the CoP corresponding to the desired GRF $\boldsymbol{f}_d$ (dotted arrow), is outside the support base, it is not admissible. When the CoP is made admissible by moving it within the support surface, the robot cannot satisfy both linear and angular momenta objectives. Two extreme solutions are illustrated. One is to fully respect linear momentum objective by sacrificing angular momentum (left) and the other is the opposite (right). One can choose a solution between the two extremes.

Fig. 4 shows two extreme cases for determining $\boldsymbol{f}$ and $\boldsymbol{p}$. The first case, left, fully respects linear momentum by laterally shifting the GRF without changing its direction, i.e., the robot puts higher priority to controlling CoM position (related to linear momentum) over body pose (related to angular momentum). As a result, given a large perturbation, rapid rotation can be generated to keep linear momentum under control. This strategy can be seen from humans when they rotate the trunk or arms forward to maintain balance given a forward push.

Fig. 4 at right, after the lateral shift, the GRF line of action is rotated to fully respect angular momentum such that $\boldsymbol{p}$ and $\boldsymbol{f}$ satisfy $\dot{\boldsymbol{k}}_d = (\boldsymbol{p} - \boldsymbol{r}_G) \times \boldsymbol{f}$. However, linear momentum is no longer respected, i.e., the robot puts higher priority to keep the desired pose (angular momentum) over its desired location (CoM). In this case, the uncontrolled linear momentum can make CoM to go too far, making it necessary to take a step in order to avoid a fall.

In this paper, we choose the first strategy to increase the capability of postural balance controller.

2) Double Support Case: Given the desired momentum rate changes, computing foot GRFs and CoPs of a double-supported robot is an under-determined problem, allowing us to impose additional optimality conditions to resolve the foot GRFs and CoPs. In this paper, we take the approach to minimize the ankle torques. A large amount of ankle torque can cause foot tipping. Hence, minimizing ankle torque is important.

Due to the presence of cross product in (2), the optimization of foot GRFs and CoPs is a nonlinear problem, which typically requires significant computation time and yet can prematurely terminate at a local minima. One way to convert this into a linear problem is to express the foot GRF and foot CoP using the contact forces at sample points [19], [18]. However, this approach increases the dimension of the search space significantly. For example, [19] used 16 variables to model a GRF and CoP of one foot, which is 10 more than the dimension of the unknowns.

Instead of increasing the search space to make the optimization problem easier, our method is to approximate the nonlinear optimization problem by sequentially solving two smaller-sized constrained linear least-squares problems, first one for determining the foot GRFs, and the next for determining the foot CoPs.

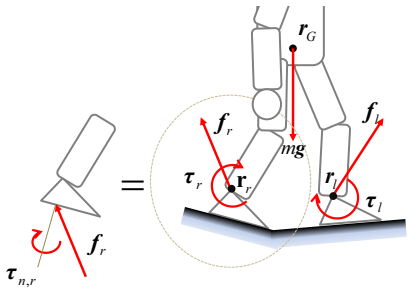

Fig. 5: By expressing foot GRF with respect to the local frame of the foot located at the ankle, we can factor out the moments $\boldsymbol{\tau}_r$, $\boldsymbol{\tau}_l$ applied to the ankle by the foot GRFs $\boldsymbol{f}_r$ and $\boldsymbol{f}_l$. $\boldsymbol{r}_r$ and $\boldsymbol{r}_l$ denote the ankle locations.

To this end, let us first rewrite (1) and (2) for the double support. Following [2], we will express the GRF at each foot with respect to the ankle (Fig. 5). The benefit of this representation is that we can explicitly express the torques applied to the ankles.

$$\dot{\boldsymbol{l}} = m\boldsymbol{g} + \boldsymbol{f}_r + \boldsymbol{f}_l \tag{5}$$

$$\dot{\boldsymbol{k}} = \dot{\boldsymbol{k}}_f + \dot{\boldsymbol{k}}_m \tag{6}$$

$$\dot{\boldsymbol{k}}_f = (\boldsymbol{r}_r - \boldsymbol{r}_G) \times \boldsymbol{f}_r + (\boldsymbol{r}_l - \boldsymbol{r}_G) \times \boldsymbol{f}_l \tag{7}$$

$$\dot{\boldsymbol{k}}_m = \boldsymbol{\tau}_r + \boldsymbol{\tau}_l \tag{8}$$

where $\boldsymbol{f}_r$ and $\boldsymbol{f}_l$ are the right and left foot GRFs, $\boldsymbol{r}_r$, $\boldsymbol{r}_l$ are the ankle locations, and $\boldsymbol{\tau}_r$, $\boldsymbol{\tau}_l$ are the ankle torques. In (6), we divide $\dot{\boldsymbol{k}}$ into two parts, $\dot{\boldsymbol{k}}_f$, due to the ankle force, and $\dot{\boldsymbol{k}}_m$, due to ankle torques.

The idea of our method is simple and intuitive. In order to minimize the ankle torques ($\dot{\boldsymbol{k}}_m \to \boldsymbol{0}$), foot GRFs $\boldsymbol{f}_r$, $\boldsymbol{f}_l$ should create $\dot{\boldsymbol{k}}_f$ as close to the desired rate of change of angular momentum ($\dot{\boldsymbol{k}}_f \to \dot{\boldsymbol{k}}_d$) as possible while satisfying $\dot{\boldsymbol{l}}_d$. If $\dot{\boldsymbol{k}}_f = \dot{\boldsymbol{k}}_d$, the ankle torques can vanish. If $\dot{\boldsymbol{k}}_f \neq \dot{\boldsymbol{k}}_d$, the ankle torques are determined to account for the residual of the angular momentum rate change, i.e., $\dot{\boldsymbol{k}}_d - \dot{\boldsymbol{k}}_f$.

a) Determination of foot GRFs: The goal is to determine the foot GRFs $\boldsymbol{f}_r$ and $\boldsymbol{f}_l$ that minimize the following objective function:

$$\min ||\dot{\boldsymbol{l}}_d - \dot{\boldsymbol{l}}|| + w||\dot{\boldsymbol{k}}_d - \dot{\boldsymbol{k}}_f|| + \epsilon(||\boldsymbol{f}_r|| + ||\boldsymbol{f}_l||) \qquad (9)$$

where $\dot{\boldsymbol{l}}$ and $\dot{\boldsymbol{k}}_f$ are the functions of $\boldsymbol{f}_r$ and $\boldsymbol{f}_l$ (eqs. (5), (7)). w and ϵ ($w \gg \epsilon > 0$) are weighting factors for the angular momentum and the total GRF magnitude, respectively. Like the single-support case, we give higher priority to linear component of the spatial momentum rate change over the angular component by setting w low.

To enforce the friction cone and unilateral force constraints, we model each GRF using four basis vectors $\boldsymbol{\beta}_{ij}$ and their magnitudes ρ_{ij} that approximate friction cone on the ground (Fig. 6)

$$\boldsymbol{f}_i = \sum_{j=1}^{4} \boldsymbol{\beta}_{ij}\rho_{ij} := \boldsymbol{\beta}_i\boldsymbol{\rho}_i \qquad (10)$$

where $\boldsymbol{\beta}_i = [\boldsymbol{\beta}_{i1} \ \cdots \ \boldsymbol{\beta}_{i4}]$. Substituting (10) into (9), we get a linear least-squares problem with simple non-negativity constraints:

$$\min ||\boldsymbol{\Phi}\boldsymbol{\rho} - \boldsymbol{\xi}|| \text{ s.t. } \boldsymbol{\rho}_i \geq 0 \qquad (11)$$

where $\boldsymbol{\rho} = [\boldsymbol{\rho}_r^T \ \boldsymbol{\rho}_l^T]^T$. $\boldsymbol{\Phi}$ and $\boldsymbol{\xi}$ are constants.[1] We solve (11) using the Non-Negative Least Squares algorithm [20], which has the merit that it does not require parameter tuning.

b) Determination of foot CoPs: After determining foot GRFs, we compute the minimal ankle torques such that they generate the residual angular momentum rate change, $\dot{\boldsymbol{k}}_{m,d} = \dot{\boldsymbol{k}}_d - \dot{\boldsymbol{k}}_f$. Since $\boldsymbol{f}_i$ is fixed, $\boldsymbol{\tau}_i$ can be written as a linear function of $\boldsymbol{d}_i$ and $\boldsymbol{\tau}_{n,i}$ (Fig. 6):

$$\boldsymbol{\tau}_i = [-\boldsymbol{f}_i]\boldsymbol{R}_i\boldsymbol{d}_i + \boldsymbol{R}_i\boldsymbol{\tau}_{n,i} \qquad (12)$$

where $\boldsymbol{R}_i$ is the orientation of a foot, so that we can express the optimization problem as a constrained least-squares problem:

$$\min ||\boldsymbol{\Psi}\boldsymbol{\eta} - \dot{\boldsymbol{k}}_{m,d}|| + \epsilon||\boldsymbol{\eta} - \boldsymbol{\eta}_d|| \text{ s.t. } \underline{\boldsymbol{\eta}} \leq \boldsymbol{\eta} \leq \overline{\boldsymbol{\eta}} \qquad (13)$$

[1] $\boldsymbol{\xi} = \begin{bmatrix}(\dot{\boldsymbol{l}}_d - m\boldsymbol{g})^T & w\dot{\boldsymbol{k}}_d^T & \boldsymbol{0}^T\end{bmatrix}^T$ and $\boldsymbol{\Phi} = \begin{bmatrix}\boldsymbol{\beta}_r & \boldsymbol{\beta}_l \\ w\boldsymbol{\delta}_r & w\boldsymbol{\delta}_l \\ & \epsilon\boldsymbol{1}\end{bmatrix}$ where $\boldsymbol{\delta}_i$ is defined as the coefficient matrix to express angular momentum rate change due to $\boldsymbol{\rho}_i$, i.e.,

$$\boldsymbol{\delta}_r\boldsymbol{\rho}_r := (\boldsymbol{r}_r - \boldsymbol{r}_G) \times \boldsymbol{f}_r = \sum_{j=1}^{4} \left((\boldsymbol{r}_r - \boldsymbol{r}_G) \times \boldsymbol{\beta}_{r,j}\right) \rho_{r,j}$$

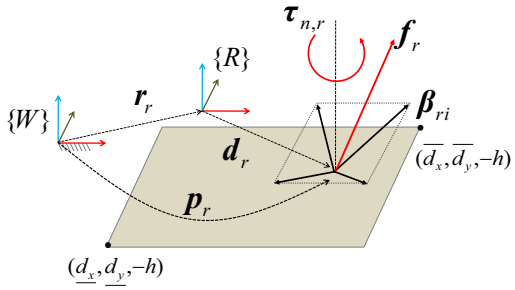

Fig. 6: We represent the ground pressure to the right foot using the foot CoP $\boldsymbol{d}_r$ in the right foot frame $\{R\}$, a normal moment $m_{n,r}$, and the foot GRF $\boldsymbol{f}_r$. $\boldsymbol{f}_r$ is represented with four basis vectors $\boldsymbol{\beta}_{rj}$ ($j = 1 \ldots 4$) that approximate the friction cone of the ground and the magnitudes ρ_{rj} (≥ 0). Therefore, the ground pressure is defined by 7 parameters, $\{\rho_{r1}, \ldots, \rho_{r4}, d_{rx}, d_{ry}, m_{n,r}\}$. This representation is compact, having only one more parameter than the minimum (3 for force and 3 for torque), and allows simple expression of the constraints for the rectangular foot support, i.e., $\rho_j \geq 0$, $\underline{d_j} \leq d_j \leq \overline{d_j}$, and $|tau_n| < \mu f_{r,z}$. μ is a friction coefficient and h is the height of foot frame from the bottom.

where $\boldsymbol{\eta} = [d_{r,x} \ d_{r,y} \ \tau_{n,r} \ d_{l,x} \ d_{l,y} \ \tau_{n,l}]^T$ is the vector of the unknowns and $\boldsymbol{\Psi} \in \mathbb{R}^{3\times 6}$ is a constant matrix of which elements are determined from (12). $\underline{\boldsymbol{\eta}}$ and $\overline{\boldsymbol{\eta}}$ are determined by the lengths of foot, and $\boldsymbol{\eta}_d$ is chosen such that $\boldsymbol{\tau}_i$ is zero (i.e., the line of action of $\boldsymbol{f}_i$ intersects the ankle). Eq. (13) is another least squares problem, but this time with upper and lower constraints. We use an implementation of Levenberg-Marquardt method [21] to solve this problem. Note that both least-squares problems have only a small number of variables, so optimization can be carried out quickly.

After determining the admissible external forces, we compute corresponding admissible momenta rate changes $\dot{\boldsymbol{k}}_a$ and $\dot{\boldsymbol{l}}_a$ from (5) and (6).

C. Joint Accelerations and Torques

The next step of the balance controller is to determine the joint accelerations $\ddot{\boldsymbol{\theta}}_a$ such that they satisfy the admissible momenta rate changes as well as the contact constraints between the foot and the ground. Finally, we compute necessary joint torques to create the joint accelerations and the external forces. For this purpose, we employ the procedures similar to [11].

$\ddot{\boldsymbol{\theta}}_a$ is determined such that it minimizes the following objective function:

$$\begin{aligned} w||\dot{\boldsymbol{h}}_a - \boldsymbol{A}\ddot{\boldsymbol{q}} - \dot{\boldsymbol{A}}\dot{\boldsymbol{q}}|| + (1-w)||\ddot{\boldsymbol{\theta}}_d - \ddot{\boldsymbol{\theta}}|| \\ \text{s.t. } \boldsymbol{J}\ddot{\boldsymbol{q}} + \dot{\boldsymbol{J}}\dot{\boldsymbol{q}} = \boldsymbol{a}_d \end{aligned} \qquad (14)$$

where $\dot{\boldsymbol{h}}_a = (\dot{\boldsymbol{k}}_a^T, \dot{\boldsymbol{l}}_a^T)^T$ is the admissible spatial momentum rate change. We use the differentiation of the centroidal spatial momentum relationship, $\boldsymbol{h} = \boldsymbol{A}\dot{\boldsymbol{q}}$ where $\boldsymbol{A} \in \mathbb{R}^{6\times(6+n)}$ is the *centroidal momentum matrix* [22] that linearly maps generalized velocities to momentum and n is the number of DoFs of the robot. $\dot{\boldsymbol{q}} = (\mathbf{v}_0, \dot{\boldsymbol{\theta}})$ is the generalized velocities where $\mathbf{v}_0 \in \mathsf{se}(3)$ is the spatial velocity of the base frame (trunk) and $\dot{\boldsymbol{\theta}} \in \mathbb{R}^n$ is the joint velocities. $\ddot{\boldsymbol{\theta}}_d$ specifies desired joint acceleration (possibly determined from a prescribed motion trajectory). $\boldsymbol{J}$ is the Jacobian matrix mapping the generalized velocities to the velocity

of the feet. w controls the importance between the balance objective and the style (or prescribed motion) objective. $\boldsymbol{a}_d = [\boldsymbol{a}_{d,r}^T \ \boldsymbol{a}_{d,l}^T]^T$ is the desired accelerations of the feet. We set $\boldsymbol{a}_d$ such that each foot has the desired configuration $\boldsymbol{T}_d \in \mathsf{SE}(3)$ and velocity $\mathbf{v}_d \in \mathsf{se}(3)$. Specifically, for each foot, we use the following feedback rule:

$$\boldsymbol{a}_{d,i} = k_p \log(\boldsymbol{T}_i^{-1}\boldsymbol{T}_{i,d}) + k_d(\mathbf{v}_{i,d} - \mathbf{v}_i) \qquad (15)$$

for $i \in \{r, l\}$ where k_p and k_d are positional and derivative feedback gains, respectively. We solve (14) by converting it to a linear equality constrained least-squares problem.

Finally, we compute feedforward torques by performing inverse dynamics. For this purpose, we use the hybrid system dynamics algorithm [23], which is useful for performing inverse dynamics for floating-base mechanisms. Since external forces are explicitly specified for all the links contacting the ground, we can treat the robot as an open loop system even when multiple links are in contact with the ground, thereby making it possible to use the inverse dynamics algorithms for open loop mechanisms.

Overall torque input is determined by adding feedback terms:

$$\boldsymbol{\tau} = \boldsymbol{\tau}_{ff} + \boldsymbol{\tau}_{fb} \qquad (16)$$

$$\boldsymbol{\tau}_{fb} = \boldsymbol{\Gamma}_p(\boldsymbol{\theta}_a - \boldsymbol{\theta}) + \boldsymbol{\Gamma}_d(\dot{\boldsymbol{\theta}}_a - \dot{\boldsymbol{\theta}}) \qquad (17)$$

where $\boldsymbol{\Gamma}_p$ and $\boldsymbol{\Gamma}_d$ are diagonal matrices representing proportional and derivative gains, respectively. $\boldsymbol{\theta}_a$ and $\dot{\boldsymbol{\theta}}_a$ are determined by numerically integrating $\ddot{\boldsymbol{\theta}}_a$ over time.

IV. Experiments and Discussion

We tested the new balance controller by simulating a humanoid robot model (Fig. 2). The total mass of the robot is 52 kg and each leg has 6 DoFs. We use the Webots software (www.cyberbotics.com) for dynamics simulation. In the experiments of this paper, we excluded the robot arms from the balance controller because arms may be engaged in other tasks to carry out simultaneously. Also, the arms are relatively lightweight to affect the state of balance significantly.

Fig. 7 shows the snapshots of the robot maintaining balance under external push (120 N, 100 ms). When the perturbation is small, the desired GRF and CoP computed from (3) and (4) are admissible and thus the robot can achieve both the desired linear and angular momentum objectives. When the perturbation is greater as shown in Fig. 7 and the controller puts higher priority to linear momentum objective, the admissible GRF and CoP are realized by generating large angular momentum. The resulting motion of the robot is similar to human's behavior of rotating the trunk in the direction of the push to maintain balance.

Fig. 8 shows trajectories of CoM, CoP, and desired/admissible momenta rate changes of this experiment. Fig. 8 (a) shows that CoM is restored smoothly after the perturbation. Right foot CoP is shown in Fig. 8 (b) and it is well maintained within the safe region defined inside the foot support. The actual foot CoP is slightly different from the admissible CoP due to the consideration of the desired motion in (14) and to the numerical error of the simulation. Fig. 8 (c) shows the desired and admissible

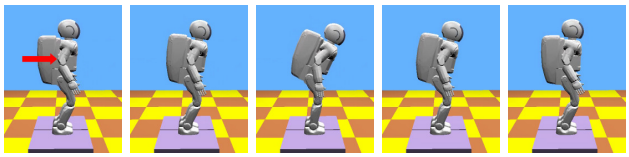

Fig. 7: Snapshots of robot balancing motion when a forward push of 120 N is applied for 100 ms to CoM of the double-support robot on the stationary support.

linear momentum rate changes and they are almost identical because the controller always respects the desired linear momentum objective. In contrast, the angular momentum is sacrificed when the desired spatial momentum rate change is not admissible (Fig. 8 (d)).

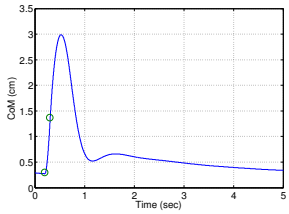

(a) CoM (forward direction)

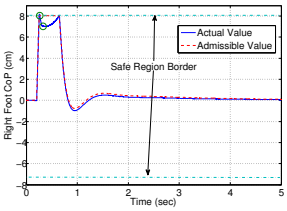

(b) Right Foot CoP (forward direction)

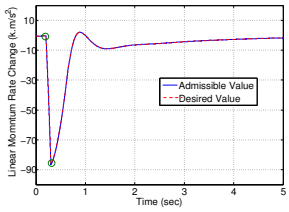

(c) Desired and Admissible Linear Momentum Rate Change (forward direction)

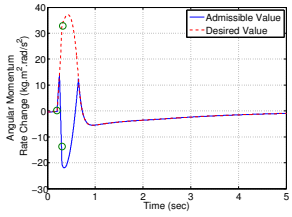

(d) Desired and Admissible Angular Momentum Rate Change (sagittal plane)

Fig. 8: Trajectories of CoM, foot CoP, and momentum rate changes for the experiment in Fig. 7. Two circles in each figure indicate the start and end of external push.

Fig. 9 (top row) shows the balance control behavior when the single-supported robot is pushed laterally. Similar to the forward push, the robot maintains balance by rotating the trunk. Although the single-supported robot has more limited range of admissible CoP than double supported case, the swing leg as well as the upper body can be employed to create larger angular momentum.

Fig. 9 (bottom row) shows the robot maintaining balance on moving supports. In this case, the perturbation from the supports is continuous and the robot shows fairly large trunk rotation. The desired CoM is set to the mid-point of the geometric centers of the two feet and its desired velocity is set to the average velocity of the feet. The supports are inclined by $\pm$ 10 deg. and they move 1 m back and forth.

The controller does not use any information on the actual direction and magnitude of the pushes or the velocity of the moving supports. In all the experiments, the following parameters were used: $\boldsymbol{\Gamma}_{11} = \mathrm{diag}\{40, 20, 40\}/m$ and $\boldsymbol{\Gamma}_{12} = \mathrm{diag}\{8, 3, 8\}/m$ in (3), $\boldsymbol{\Gamma}_{21} = \mathrm{diag}\{20, 20, 20\}$ in (4), $w = 0.1$, $\epsilon = 0.01$ in (9), and $\epsilon = 0.01$ in (13).

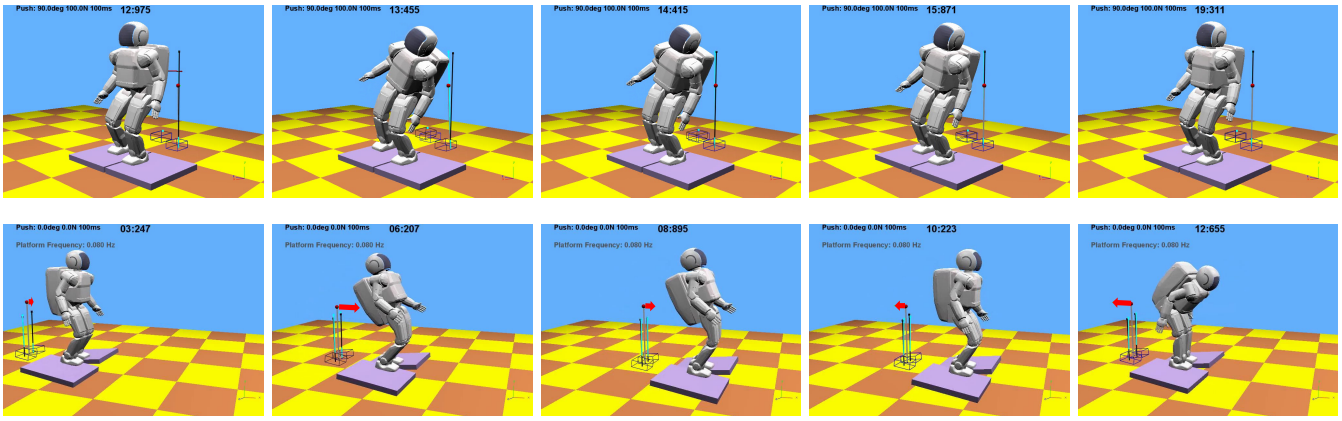

Fig. 9: Top: A leftward push (100 N, 100 ms) is applied to the single-support robot on the stationary ground. The robot maintains perturbation by counter-rotating the upper body. Bottom: Two moving supports with different inclination angles translate forward and backward in a sinusoidal pattern, and the robot keeps balance by rotating its upper body. The red arrows indicate the linear momentum of the robot.

V. Conclusion and Future Work

In this paper, we introduced a novel balance control method for humanoid robots on non-level, non-continuous, and non-stationary grounds. By controlling both linear and angular momentum of the robot, this whole body balance controller can maintain balance under relatively large perturbations and often generates human-like balancing behavior. A distinctive feature of our method is that, by determining the CoP and GRF at each support foot without using the traditional net CoP and net GRF of the robot, the controller can deal with different ground geometry and ground frictions at each foot. We showed the performance of the balance controller through a number of simulation experiments.

In this work, we give higher priority to linear momentum over angular momentum. While this is a sensible choice for a postural balance controller, a more robust balance controller will be possible if we find an optimal balance between the two, which remains as a promising venue of future work.

References

[1] M. Vukobratović and D. Juričić, "Contribution to the synthesis of biped gait," *IEEE Trans. Bio-Medical Eng.*, vol. 16, no. 1, 1969.

[2] A. Sano and J. Furusho, "Realization of natural dynamic walking using the angular momentum information," in *IEEE Intn'l Conf. on Robotics and Automation (ICRA)*, May 1990, pp. 1476 – 1481.

[3] B. Stephens, "Integral control of humanoid balance," in *IEEE/RSJ Intn'l Conf. on Intelligent Robots and Systems (IROS)*, 2007.

[4] S. Kagami, F. Kanehiro, Y. Tamiya, M. Inaba, and H. Inoue, "AutoBalancer: An online dynamic balance compensation scheme for humanoid robots," in *Proc. of the 4th Inter. Workshop on Algorithmic Foundation on Robotics*, 2000.

[5] T. Sugihara, Y. Nakamura, and H. Inoue, "Realtime humanoid motion generation through ZMP manipulation based on inverted pendulum control," in *icra*, May 2002, pp. 1404–1409.

[6] S. Kajita, F. Kanehiro, K. Kaneko, K. Fujiwara, K. Harada, K. Yokoi, and H. Hirukawa, "Resolved momentum control: Humanoid motion planning based on the linear and angular momentum," in *IEEE/RSJ Intn'l Conf. on Intelligent Robots and Systems (IROS)*, vol. 2, 2003, Las Vegas, NV, USA, pp. 1644–1650.

[7] Y. Choi, D. Kim, Y. Oh, and B.-J. You, "Posture/walking control for humanoid robot based on kinematic resolution of CoM Jacobian with embedded motion," *IEEE Trans. on Robotics*, vol. 23, no. 6, pp. 1285–1293, 2007.

[8] Y. Abe, M. da Silva, and J. Popović, "Multiobjective control with frictional contacts," in *SCA '07: Proceedings of the 2007 ACM SIGGRAPH/Eurographics symposium on Computer animation*, 2007, pp. 249–258.

[9] C. Zhou and Q. Meng, "Dynamic balance of a biped robot using fuzzy reinforcement learning agents," *Fuzzy Sets and Systems*, vol. 134, no. 1, pp. 169–187, 2003.

[10] T. Komura, H. Leung, S. Kudoh, and J. Kuffner, "A feedback controller for biped humanoids that can counteract large perturbations during gait," in *IEEE Intn'l Conf. on Robotics and Automation (ICRA)*, 2005, Barcelona, Spain, pp. 2001–2007.

[11] A. Macchietto, V. Zordan, and C. R. Shelton, "Momentum control for balance," *ACM Transactions on Graphics*, vol. 28, no. 3, pp. 80:1–80:8, July 2009.

[12] M. Popovic, A. Hofmann, and H. Herr, "Angular momentum regulation during human walking: Biomechanics and control,," in *IEEE Intn'l Conf. on Robotics and Automation (ICRA)*, April, New Orleans, LA, USA 2004, pp. 2405–2411.

[13] A. Goswami and V. Kallem, "Rate of change of angular momentum and balance maintenance of biped robots," in *IEEE Intn'l Conf. on Robotics and Automation (ICRA)*, April 2004, pp. 3785–3790.

[14] S. Kajita, T. Yamaura, and A. Kobayashi, "Dynamic walk control of a biped robot along the potential energy conserving orbit," *IEEE Trans. on Robotics and Automation*, vol. 8, no. 4, pp. 431–438, 1992.

[15] N. Naksuk, Y. Mei, and C. Lee, "Humanoid trajectory generation: an iterative approach based on movement and angular momentum criteria," in *IEEE/RAS Intn'l Conf. on Humanoid Robots*, Nov. 2004, pp. 576–591.

[16] M. Abdallah and A. Goswami, "A biomechanically motivated two-phase strategy for biped robot upright balance control," in *IEEE Intn'l Conf. on Robotics and Automation (ICRA)*, April 2005, Barcelona, Spain, pp. 3707–3713.

[17] A. Hofmann, M. Popovic, and H. Herr, "Exploiting angular momentum to enhance bipedal center-of-mass control," in *IEEE Intn'l Conf. on Robotics and Automation (ICRA)*, May 2009, pp. 4423–4429.

[18] S.-H. Hyon, J. Hale, and G. Cheng, "Full-body compliant human–humanoid interaction: Balancing in the presence of unknown external forces," *IEEE Trans. on Robotics*, vol. 23, no. 5, pp. 884–898, Oct. 2007.

[19] N. S. Pollard and P. S. A. Reitsma, "Animation of humanlike characters: Dynamic motion filtering with a physically plausible contact model," in *Yale Workshop on Adaptive and Learning Systems*, 2001.

[20] C. L. Lawson and R. J. Hanson, *Solving least squares problems*. Prentice-Hall, 1974.

[21] M. Lourakis, "levmar: Levenberg-Marquardt nonlinear least squares algorithms in C/C++," http://www.ics.forth.gr/ lourakis/levmar/, Jul. 2004.

[22] D. Orin and A. Goswami, "Centroidal momentum matrix of a humanoid robot: Structure and properties," in *IEEE/RSJ Intn'l Conf. on Intelligent Robots and Systems (IROS)*, 2008, Nice, France.

[23] R. Featherstone, *Robot Dynamics Algorithms*. Kluwer Academic Publishers, 1987.